An MRI Estimate of Vascular Permeability in 9L Cerebral Tumor Agrees with Those of Quantitative Autoradiography

J. R. Ewing[1,2], T. N. Nagaraja[3], R. paudyal[4], H. Bagher-Ebadian[1,5], K. Robert[1], L. Karyn[1], and J. D. Fenstermacher[3]

[1]Neurology, Henry Ford Hospital, Detroit, MI, United States, [2]Physics, Oakland University, Rochester, MI, United States, [3]Anesthesiology, Henry Ford Hospital, Detroit, MI, United States, [4]physics, oakland University, rochester, mI, United States, [5]Physics and Nuclear Engineering, Amir-Kabir University of Technology, Tehran, Iran

Introduction: Quantitative estimates of vascular permeability, in the form of maps of the vascular transfer constant, K_1 (or K^{trans}) for a contrast agent (CA), are becoming important in clinical studies of solid tumors, particularly in assessing response to antiangiogenic therapy (c.f. Batchelor *et al*[1]). These techniques generally utilize the 'standard,' or 'Tofts' model and, because of restricted intra- to extra-cellular (ic to ec) water exchange, produce estimates that can be biased low[2] by as much as 300%. Contrariwise, the extended models necessary to account for finite ic to ec water exchange rates are overdetermined and, with attainable MRI signal-to-noise, will not produce stable estimates[3] of the 5 parameters[2] necessary to estimate K_1: in order to achieve stability, these approaches must set some parameters constant, and will thereby also introduce a bias in the remaining parametric estimates. In short, the typical biases of widely used techniques for estimating K_1 are currently unknown. In this setting, a technique that produces an unbiased MRI estimate of K_1 can serve as a validation reference to characterize the biases of other methods. We have developed such a technique and used nearly identical CAs - Gd-DTPA-labeled albumin (Gd-BSA) and radioiodinated serum albumin (RISA) – to map K_1 in the same animal. Herein we present the agreement in estimating K_1 between the MRI estimate and that of quantitative autoradiography (QAR).

Materials and Methods: ***MRI Experimental:*** 15 Fisher 344 rats with cerebrally implanted 9L tumor[4] were studied. Mean tumor age was 14.6 ± 0.7 days (range 14 to 16 days). MRI took place in a 7 Tesla magnet for small-animal imaging, interfaced to a Bruker Avance console running Paravision V 3.0.2, and using a Bruker volume resonator and 2 cm surface coil pair. CA concentration was followed via a Look-Locker[6] (LL) sequence Following a non-selective adiabatic pulse to invert the magnetization, one phase-encode line of 24 small-tip-angle pulses (~ 18º, TE 4 ms) was acquired at 50 ms intervals, for a total recovery time of 1200 ms with a 2.2 sec TR. Matrix size was 128X64, FOV 32 mm, three 2 mm slices. Prior to CA administration, two baseline LL studies were obtained. After CA administration (140 µM Gd-BSA in 0.5 ml, slow IV push over ~ 1 min), 10 LL sequences were run to follow tissue concentration of CA across 25 minutes. Afterward, pixel-by-pixel R_1 ($R_1 = 1/T_1$) maps were constructed[7]. Post- minus pre-contrast changes in R_1 (ΔR_1) were employed as estimates of CA concentration in blood and tissue, utilizing the sagittal sinus as an estimate of blood CA concentration. Maps of K_1 were constructed (see "MRI K_1" section below). A post-contrast high-resolution T_1-weighted image was used to form regions of interest (ROIs) for later analysis.

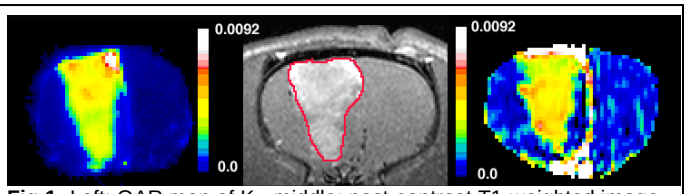

Fig 1: Left: QAR map of K_1, middle: post-contrast T1-weighted image with ROI. Right: MRI map of K_1.

$$C_t(t_t) = K_1 \int_0^{t_t} C_p(\tau)\, d\tau \qquad \textbf{Eq 1}$$

QAR Theory: QAR estimates of K_1 are single-point estimates taken at the time point of decapitation. The model assumes that there is no efflux of tracer once it has entered the tissue, and ignores the vascular component of tracer in the tissue. The model equation (Eq 1) is a variant of the Patlak model[8], where $C_t(t)$ is the time-varying tissue concentration of indicator, $C_p(t)$ is the plasma concentration, and t_t is the termination time of the experiment.

QAR Experimental: Immediately after MRI, the anesthetized rats were removed from MRI and prepared for QAR, as in Bagher-Ebadian et al[9]. A femoral artery was cannulated, and ~ 100 µCi of radioiodinated (^{125}I) bovine serum albumin (RISA) in 1 ml normal saline was injected through the tail vein as a slow bolus over a minute, as in the MRI injection of Gd-BSA. Timed arterial blood samples were obtained to establish the arterial input curve. Thirty minutes after the bolus injection, the rat was decapitated and the head was immediately frozen[10,11]. The frozen brain was then cut into a series of five 20 µm thick sections at 200 µm intervals. These sections and a set of ^{125}I standards were exposed to imaging film for 7-10 days to obtain the autoradiograms, producing estimates of tissue concentration.

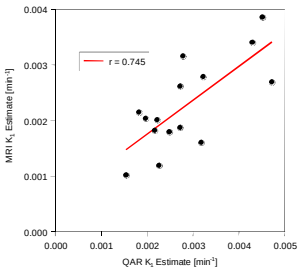

Fig 2: MRI estimates of the transfer constant for albumin in a 9L cerebral tumor (ordinate) versus QAR estimates.

The autoradiograph contact sheet was examined and 3 to 5 slices were chosen to match the anatomy of the selected MRI slice. The selected autoradiographic slices were then co-registered, and averaged across all the slices, producing an averaged autoradiograph that corresponded to the MRI slice. This averaged autoradiogram was then co-registered to the MRI slice. Finally, using the averaged activity, the calibration standards, and the time record of plasma activity, the QAR map of K_1 was calculated pixel-by-pixel using Eq 1.

MRI K_1: Using the same assumptions as that of the QAR procedures (Eq 1), MRI estimates of K_1 were also calculated. To assure that the two techniques used the same estimate for $C_p(t)$, the QAR plasma concentration of RISA was scaled to the sagittal sinus ΔR1 curve and used as the input function. The K_1 values from the selected ROIs were recorded and then plotted on a scatter plot for correlation analysis (Fig 2).

Results and Discussion: Visually, the MRI and QAR maps of K_1 strongly resembled each other (Fig 1). In 15 ROIs selected, the QAR and MRI estimates were not significantly different in their means; mean QAR K_1 = $(2.26 \pm 0.80)X10^{-3}$ [min^{-1}], mean MRI K_1 = $(2.85 \pm 0.98)X10^{-3}$ [min^{-1}] ($t = -1.80$, $p = 0.08$). The two measures were well-correlated ($r = 0.745$, $p < 0.001$) (Fig 2). Considering the difficulties in co-registration, which we believe were the main source of systematic error, this degree of correlation implies that the two measures of transfer constant are in essential agreement.

Conclusion: MRI maps of K_1 using LL measures of ΔR_1 yield estimates of of K_1 that are not significantly different from that of a classical measure of that parameter. We conclude that MRI maps of K_1 using LL measures of ΔR_1, where $K_1 < 1X10^{-2}$ [min^{-1}] yield unbiased estimates of the transfer constant, and that the MRI maps of K_1 thus produced can be taken as a standard in MRI estimates of vascular permeability.

Literature Cited: 1. Batchelor, T.T., et al., Cancer Cell, 2007. **11**(1): p. 83. **2.** Yankeelov, T.E., et al., Magn Reson Imag, 2007. **25**(1): p. 1. **3.** Quirk, J.D., et al., MRM, 2003. **50**: p. 493. **4.** Ewing, J.R., et al., J Cereb Blood Flow Metab, 2006. **26**(3): p. 310. **5.** Nagaraja, T.N., et al., J Neurosci Methods, 2006. **157**(2): p. 238. **6.** Brix, G., et al., Magn Reson Imag, 1990. **8**: p. 351. **7.** Williams, L.A., et al., Radiology, 2005. **235**(2): p. 595. **8.** Patlak, C.S., et al., J Cereb Blood Flow Metab, 1983. **3**: p. 1. **9.** Bagher-Ebadian, H., et al., MRM, 2007. **58**(2): p. 290. **10.** Blasberg, R.G., et al., J Cereb Blood Flow Metab, 1983. **3**: p. 8. **11.** Nakagawa, H., et al., J Cereb Blood Flow Metab, 1987. **7**: p. 687.